


Correlation Between Dynamic Contrast-Enhanced CT Imaging Signs and Differentiation Grade and Microvascular Invasion of Hepatocellular Carcinoma

Yang Liu ^{1,2}, Yunhui Zhou³, Cong Liao^{1,2}, Hang Li², Xiaolan Zhang⁴, Haigang Gong⁵, Hong Pu^{1,2}

¹School of Medicine, University of Electronic Science and Technology, Sichuan, China; ²Department of Radiology, Sichuan Academy of Medical Sciences & Sichuan Provincial People's Hospital, Sichuan, People's Republic of China; ³Department of Radiology, Chengdu Pidu District People's Hospital, Sichuan, People's Republic of China; ⁴Shukun Technology Co., Ltd, Beijing, People's Republic of China; ⁵School of Computer Science and Engineering, University of Electronic Science and Technology, Sichuan, People's Republic of China

Correspondence: Hong Pu, Department of Radiology, Sichuan Academy of Medical Sciences, Sichuan Provincial People's Hospital; School of Medicine, University of Electronic Science and Technology, Chengdu, Sichuan Province, 610000, People's Republic of China, Email ph196797@163.com; Haigang Gong, School of Computer Science and Engineering, University of Electronic Science and Technology, Chengdu, Sichuan Province, 610000, People's Republic of China, Email hggong@uestc.edu.cn

Objective: This study aimed to investigate how dynamic contrast-enhanced CT imaging signs correlate with the differentiation grade and microvascular invasion (MVI) of hepatocellular carcinoma (HCC), and to assess their predictive value for MVI when combined with clinical characteristics.

Methods: We conducted a retrospective analysis of clinical data from 232 patients diagnosed with HCC at our hospital between 2021 and 2022. All patients underwent preoperative enhanced CT scans, laboratory tests, and postoperative pathological examinations. Among the 232 patients, 89 were identified as MVI-positive and 143 as MVI-negative. Regarding tumor differentiation, 56 patients were well-differentiated, 145 moderately, and 31 poorly. Multivariate logistic regression analysis was employed to establish a prediction model for variables showing significant differences. Additionally, the diagnostic performance of various indicators were evaluated using ROC analysis.

Results: Among the qualitative data, significant differences ($P < 0.05$) were observed between the MVI-positive and MVI-negative groups in 5 items such as peritumoral enhancement. In terms of quantitative data, the MVI-positive group exhibited higher maximum tumor length, AST, ALT, AFP levels and the ALBI score ($P < 0.05$). Conversely, CT values in the arterial phase (AP), portal venous phase (PVP), and PT levels were lower in the MVI-positive group ($P < 0.05$). Multivariate Logistic regression analysis identified ALBI score, PT level, CT value in PVP, and tumor capsule as independent risk factors for MVI occurrence (AUC: 0.71, 0.58, 0.66, and 0.60). The combined diagnostic AUC value was 0.82 (95% CI: 0.76–0.87). Significant differences were found among different differentiation grade groups in 10 items such as non-smooth tumor margin ($P < 0.05$).

Conclusion: Preoperative dynamic contrast-enhanced CT examination in patients with HCC can be utilized to predict the presence of MVI. When combined with clinical characteristics, these imaging signs demonstrate good predictive performance for MVI status. Furthermore, this approach has significant implications for determining the differentiation grade of tumors.

Keywords: hepatocellular carcinoma, microvascular invasion, computed tomography, differentiation grade

Introduction

Primary liver cancer (PLC) is a prevalent malignant tumor of the digestive system, ranking fourth in terms of new cancer cases, yet it holds the second position among causes of death.¹ Among PLCs, hepatocellular carcinoma (HCC) constitutes approximately 75% to 85%.^{2,3} The recurrence rate after HCC surgery can be as high as 50% to 70% within five years.⁴ Key factors influencing the biological behavior of HCC include microvascular invasion (MVI) and the degree

of tumor differentiation, known as histological grade.^{5,6} The incidence of MVI in HCC can range from 15% to 57%.^{7,8} Its presence indicates a more aggressive biological behavior of the tumor with increased risk of metastasis, serving as an independent prognostic factor affecting both early recurrence and long-term survival rates following surgery.^{7,8} Predicting MVI preoperatively holds significant importance for precise treatment strategies in HCC patients. Radiofrequency ablation (RFA) is recommended by the European Association for the Study of the Liver (EASL) clinical practice guidelines (2018) as a first-line treatment for small liver cancers, offering an alternative to surgical resection. However, RFA is not advised for patients with MVI-positive tumors due to a higher recurrence risk compared to surgical resection.^{9,10} The degree of pathological differentiation in HCC significantly impacts patient prognosis, with poorer clinical outcomes associated with lower differentiation levels.^{11,12} Currently, the definitive diagnosis of MVI status and tumor pathological staging typically relies on postoperative histopathological examination. However, this approach hinders the timely formulation of treatment plans and assessment of postoperative survival. Therefore, non-invasive and rapid preoperative evaluation of MVI status and tumor differentiation grade holds immense value. Such evaluations are crucial for selecting appropriate treatment strategies, predicting disease progression, and enhancing overall survival rates.

In patients with abnormal liver ultrasound findings or elevated alpha-fetoprotein (AFP) levels, dynamic contrast-enhanced CT plays a crucial role as a primary imaging method in diagnosing HCC. It holds significant research value in evaluating the pathological information of HCC.^{7,11,12} Currently, there is a lack of comprehensive evaluation of the traditional imaging features and clinical factors related to the differentiation and MVI in HCC.^{7,11,12} Our study aimed to explore the correlation between dynamic contrast-enhanced CT imaging signs and the pathological grade of HCC, as well as the status of MVI.

Materials and Methods

Patients and Materials

The clinical data of 232 patients diagnosed with HCC who underwent surgery in Sichuan Provincial People's Hospital between January 1, 2021 and December 31, 2022 were analyzed retrospectively. All patients received confirmation of HCC through postoperative pathology. The study received ethical approval from the hospital's Ethics Committee, and informed consent was waived.

Inclusion criteria were as follows:¹ Dynamic contrast-enhanced CT examination conducted within 2 weeks before surgery with acceptable image quality;² Pathologically confirmed MVI and tumor differentiation results;³ Complete preoperative clinical markers data. Exclusion criteria included:¹ History of prior liver surgery, transcatheter arterial chemoembolization, radiofrequency ablation, or systemic chemotherapy;² Presence of recurrent or metastatic tumors;³ Evidence of macroscopic vascular invasion or extrahepatic metastasis on CT images;⁴ Extensive tumor necrosis.⁵ For multifocal HCC, non-largest tumors were proven to be MVI (+).

Clinical data encompassed demographic details such as age, gender, pathological diagnosis of liver cirrhosis, hepatitis virus infection status, and serological markers.

Acquisition Protocol

The standardized scanning of multiphase imaging was emphasized, the same imaging parameters, scanning protocols and data analysis methods were adopted to ensure the comparability of different imaging results. A Siemens SOMATOM Perspective 64-slice CT scanner was used with the following parameters: tube voltage 120kV, tube current 104mAs. Patients were scanned in a supine position, after a 6–8 hour fast. The scan range extended from the diaphragmatic dome to the inferior liver pole. The scan protocol included a non-contrast scan, followed by intravenous injection of the contrast agent iohexol injection (iodine content 300 mg I/mL) at a rate of 2.5 mL/s, with doses calculated at 1.0 mL/kg of body weight. Late arterial phase (AP), portal venous phase (PVP), and delayed phase (DP) scans were performed 35s, 60s, and 3 minutes post-contrast injection, respectively. Images were reconstructed with a slice thickness of 2–5 mm, and an interslice distance of 0.625 mm, using a standard reconstruction algorithm.

Image Analysis

The images underwent post-processing on the Siemens SyngoVia workstation. The evaluation was conducted by two radiologists with 3 years and 30 years of experience, respectively. They performed the analysis without prior knowledge of the patients' clinical information, serological markers, or histopathological results. A re-check was carried out two weeks later. Both doctors were members of the research group, and the junior doctor also had read more than 2000 liver CT studies. Before the study, they received practical guidance together and mastered the structural liver imaging scoring system proficiently. After training, practical cases from the imaging system were randomly selected for assessment. In case of disagreement between the two radiologists, the results of discussion shall prevail. When there is still disagreement, it will be examined by another radiologist with 30 years of experience in liver image-reading. The two radiologists assessed the following imaging features:¹ Quantitative data: They selected the transverse section of the largest tumor in the late AP and PVP, measuring the maximum tumor length, average CT values in AP and PVP, while excluding visible blood vessels, bile ducts, cystic degeneration, necrosis, bleeding, and artifacts.² Qualitative data: Tumor margin, peritumoral enhancement, intratumoral artery, tumor capsule, peritumoral hypodensity, typical enhancement patterns, cyst degeneration/necrosis. For multifocal HCC, the analysis focused on the largest tumor.

Pathological Diagnosis

According to the Standardized Pathological Diagnosis Guidelines for Primary Liver Cancer (2015 Edition),^{13,14} specimens were obtained and diagnosed. In cases where microvascular thrombosis was identified under the microscope, it was categorized as MVI-positive; otherwise, it was categorized as MVI-negative. Pathological grading was performed according to the WHO-recommended method of high, moderate, and low differentiation. Evaluation of each patient's tumor histopathological characteristics, including pathological findings, differentiation grade, MVI status, and peritumoral cirrhosis, was conducted by one junior and one senior pathologist, who had access to clinical information. In cases of discordance in results, a consensus was reached through discussion between the two pathologists.

Statistic Analysis

Statistical analysis was conducted using SPSS Statistics 28.0 software. Cohen's kappa was used to evaluate interobserver agreement on image features. Features with substantial or nearly perfect interobserver agreement ($\kappa > 0.6$) were selected for inclusion in the research. Quantitative data were presented as mean \pm standard deviation ($\bar{x} \pm s$). The *T*-test was employed for comparisons between two groups, while one-way ANOVA was utilized for comparisons among multiple groups. For non-normally distributed data, median and Interquartile Range (IQR) (M (P25, P75)) were used, with the Mann-Whitney *U*-test for two-group comparisons and the Kruskal-Wallis *H*-test for comparisons among multiple groups. Qualitative data were expressed as frequencies (n) and percentages (%). Pearson's chi-square test or Fisher's exact test was used for comparisons of non-ordered categorical variables, and the rank-sum test was used for ordinal categorical variables. Multivariate logistic regression analysis was performed to identify independent risk factors associated with MVI. The area under the curve (AUC) of the receiver operating characteristic (ROC) curve was used as an evaluation index, with corresponding sensitivity, specificity, positive predictive value, and negative predictive value calculated. A significance level of $P < 0.05$ was considered statistically significant.

Results

Patient Characteristics

According to the histopathological results, the patients were divided into the MVI (+) group (89 cases) and the MVI (-) group (143 cases). There were no significant differences in gender, age, HBV infection, and liver cirrhosis between the MVI (+) and MVI (-) groups ($P > 0.05$) (Table 1). According to the histopathological results, the patients were divided into well differentiated (56 cases), moderately differentiated (145 cases), and poorly differentiated (31 cases) groups. There were no significant differences in gender, age, HBV infection, and liver cirrhosis between the groups ($P > 0.05$) (Table 2).

Table 1 Comparison of Characteristics Between the MVI (+) Group and the MVI (-) Group

Characteristics	MVI (+) (n=89)	MVI (-) (n=143)	χ^2/t	P value
Sex			0.031	0.861
Male	72(80.9)	117(81.8)		
Female	17(19.1)	26(18.2)		
Age (y)	58.2±10.7	59.6±12.0	0.901	0.369
HBsAg			0.387	0.534
Positive	68(76.4)	104(72.7)		
Negative	21(23.6)	39(27.3)		
Cirrhosis			1.8	0.18
Yes	52(58.4)	96(67.1)		
No	37(41.6)	47(32.9)		

Notes: Unless otherwise specified, data in the tables represent patient counts, with percentages in parentheses. *Data are presented as mean ± standard deviation.

Table 2 Comparison of Characteristics of Well, Moderately, and Poorly Differentiated Groups

Characteristics	Well (n=56)	Moderate (n=145)	Poorly (n=31)	P value
Sex				0.794
Male	44(78.6)	119(82.1)	26(83.9)	
Female	12(21.4)	26(17.9)	5(16.1)	
Age (y)	60.4±9.9	58.4±12.2	59.6±11.0	0.506
HBsAg				0.145
Positive	38(67.6)	107(73.8)	27(87.1)	
Negative	18(32.1)	38(26.2)	4(12.9)	
Cirrhosis				0.532
Yes	37(66.1)	94(64.8)	17(54.8)	
No	19(33.9)	51(35.2)	14(45.2)	

Dynamic Contrast-Enhanced CT Imaging Signs of HCC

Dynamic contrast-enhanced CT images revealed the characteristic enhancement pattern of HCC: hyperenhancement in the AP and washout appearance in the PVP and/or DP compared to the surrounding liver tissue (Figure 1A–C). Among the study participants, 206 (89%) exhibited this typical enhancement pattern. Additionally, 169 (73%) patients presented with a tumor capsule (Figure 1C), 102 (44%) had an irregular tumor margin (Figure 1D and E), 155 (67%) showed intratumoral arteries (Figure 1F), 35 (15%) displayed peritumoral enhancement (Figure 1G), 91 (39%) had peritumoral hypodensity (Figure 1H), and 161 (70%) exhibited cystic degeneration or necrosis (Figure 1I).

Comparison of Dynamic Contrast-Enhanced CT Image Signs Between the MVI (+) Group and the MVI (-) Group

There were statistically significant differences in tumor margin, peritumoral enhancement, cystic degeneration or necrosis, tumor capsule, maximum tumor length, CT values in AP and PVP between MVI-positive and negative groups ($P < 0.05$). There were no significant differences in the intratumoral artery, peritumoral hypodensity, and typical enhancement pattern between the two groups ($P > 0.05$) (Table 3 and Figure 2).

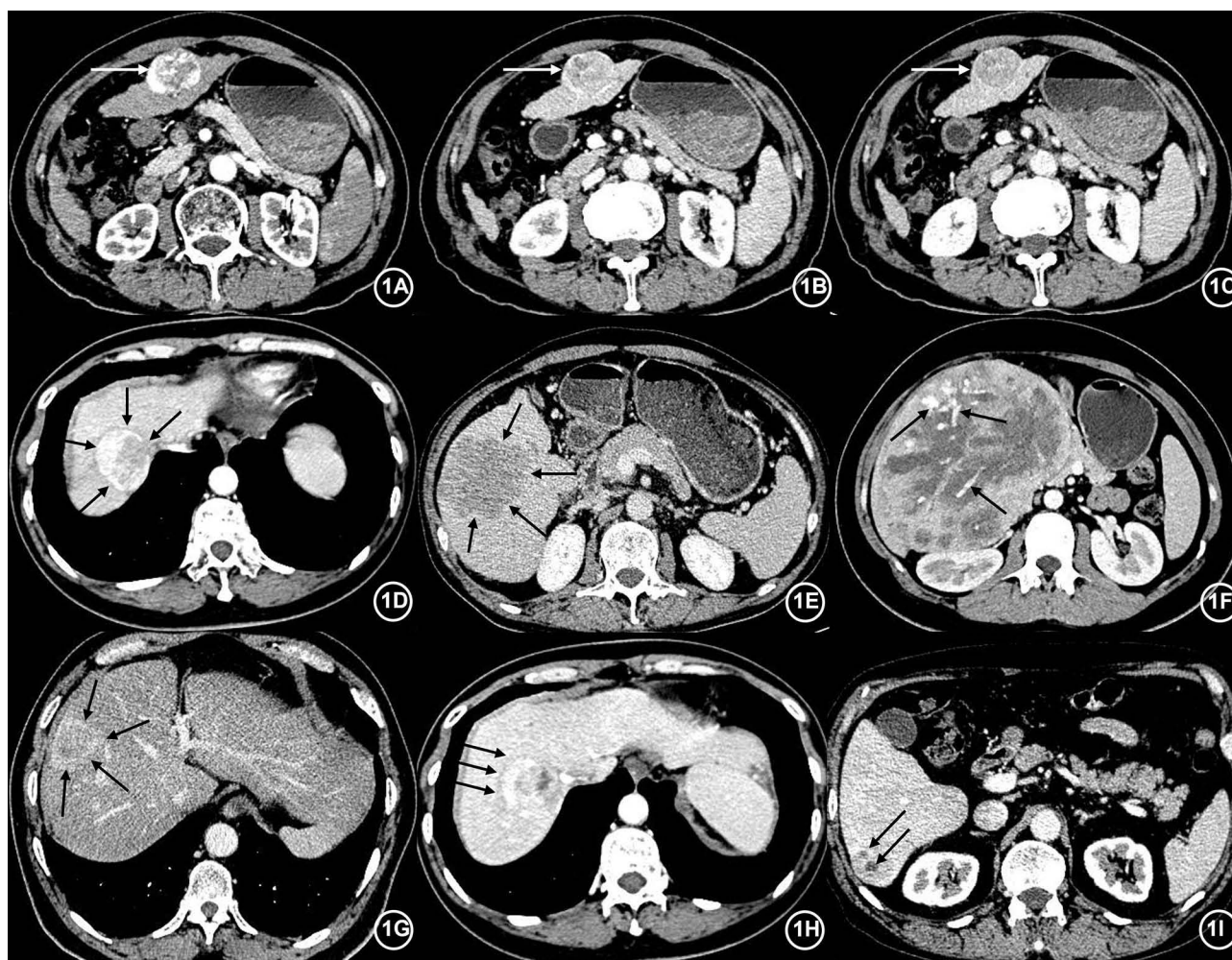


Figure 1 (1A–1C) show the typical enhancement pattern of HCC, known as “rapid enhancement and rapid washout” (white arrows); (1D and 1E) represent smooth and irregular tumor margins, respectively (black arrows); (1F) displays the intratumoral arteries of HCC (black arrow); (1G) illustrates peritumoral enhancement in HCC (black arrow); (1H) demonstrates peritumoral hypodensity in HCC (black arrow); (1I) reveals cystic degeneration or necrosis areas in HCC (black arrow).

Comparison of Dynamic Contrast-Enhanced CT Image Indicators Between Well, Moderately, and Poorly Differentiated Groups

There were statistically significant differences in the smooth margin, tumor capsule, peritumoral hypodensity, typical enhancement pattern, CT value in AP, CT value in PVP, and maximum diameter among the different differentiation grade groups ($P < 0.05$). There was no significant difference in peritumoral enhancement, intratumoral artery, cyst degeneration, or necrosis between the groups ($P > 0.05$) (Table 4 and Figure 3).

Table 3 Comparison of Contrast-Enhanced CT Image Signs Between MVI (+) Group and MVI (-) Group

Characteristics	MVI (+) (n=89)	MVI (-) (n=143)	Statistic	P value
Qualitative indicators				
Tumor margin			16.363	<0.001
Smooth	35(39.3)	95(66.4)		
Irregular	54(60.7)	48(33.6)		
Peritumoral enhancement			8.162	0.004
Yes	21(23.6)	14(9.8)		
No	68(76.4)	129(90.2)		

(Continued)

Table 3 (Continued).

Characteristics	MVI (+) (n=89)	MVI (-) (n=143)	Statistic	P value
Intratumoral artery			3.135	0.077
Yes	66(74.2)	90(62.9)		
No	23(25.8)	53(37.1)		
Tumor capsule			10.812	0.001
Yes	54(60.7)	115(80.4)		
No	35(39.3)	28(19.6)		
Peritumoral hypodensity			0.179	0.672
Yes	33(37.1)	57(39.9)		
No	56(62.9)	86(60.1)		
Typical enhancement			1.677	0.195
Yes	76(85.4)	130(90.9)		
No	13(14.6)	13(9.1)		
Cystic degeneration or necrosis			8.4	0.004
Yes	72(80.9)	90(62.9)		
No	17(19.1)	53(37.1)		
Quantitative indicators				
CT values in AP (Hu)	71(62.5, 87.0)	83.0(71.8, 95.5)	-3.735	<0.001
CT values in PVP (Hu)	76.0(66.5, 86.5)	85.0(75.8, 94.3)	-4.132	<0.001
Maximum tumor length (mm)	54(34, 85)	39(28, 64)	-3.378	0.001

Note: *Data are for median and IQR.

Other Clinical Factors Influencing HCC MVI or Pathologic Grade

The levels of AST, ALT, AFP, ALBI score, and worse differentiation in the MVI (+) group were significantly higher than those in the MVI (-) group, and the PT level in the MVI (+) group was lower than those in the MVI (-) group, with a

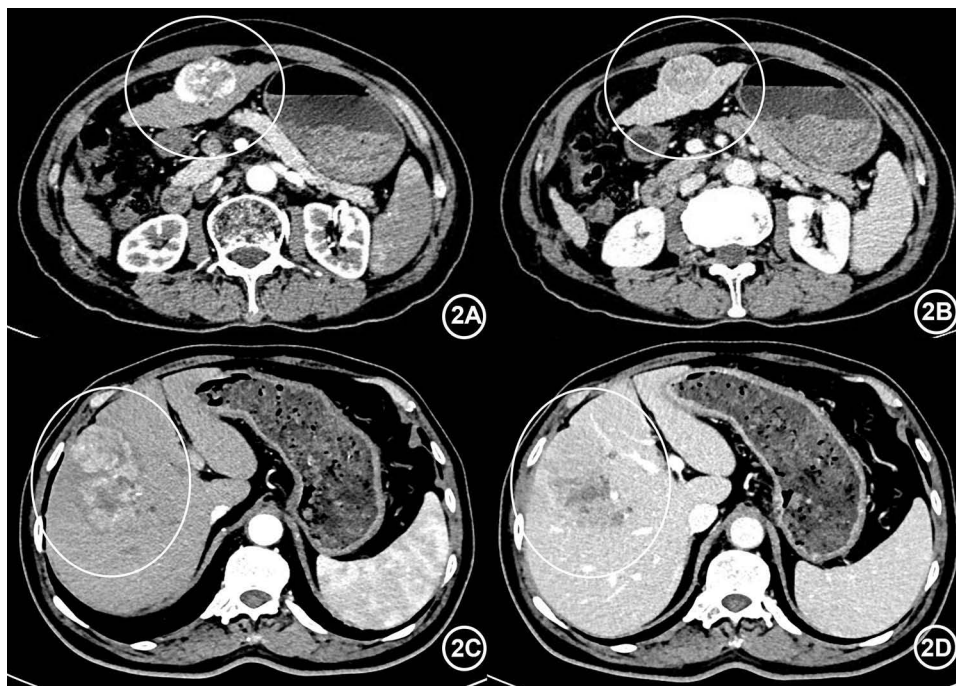


Figure 2 MVI-related imaging. (2A and 2B) A 82-year-old man with HCC, MVI (-). AP (2A) and PVP (2B) images show smooth tumor margin, tumor capsule, intratumoral artery, and typical enhancement pattern. The maximum tumor length is 41mm. The CT value in AP and PVP are 157Hu and 104Hu respectively. (2C and 2D): A 65-year-old man with HCC, MVI (+). AP (2C) and PVP (2D) images show irregular tumor margin, intratumoral artery, cystic, degeneration or necrosis, and typical enhancement pattern. The maximum tumor length is 76mm. The CT value in AP and PVP are 97Hu and 104Hu respectively.

Table 4 Comparison of Contrast-Enhanced CT Image Indicators Among Well, Moderately, and Poorly Differentiated Groups

Characteristics	Well (n=56)	Moderately (n=145)	Poorly (n=31)	P value
Qualitative indicators				
Smooth margin				0.002
Smooth	40(71.4)	80(55.2)	10(32.3)	
Unsmooth	16(28.6)	65(44.8)	21(67.7)	
Peritumoral enhancement				0.061
Yes	4(7.1)	23(15.9)	8(25.8)	
No	52(92.1)	123(84.1)	23(74.2)	
Intratumoral artery				0.304
Yes	33(58.9)	102(70.3)	21(67.7)	
No	23(41.1)	43(29.7)	10(32.3)	
Tumor capsule				0.014
Yes	47(83.9)	105(72.4)	17(54.8)	
No	9(16.1)	40(27.6)	14(45.2)	
Peritumoral hypodensity				0.02
Yes	28(50.0)	56(38.6)	6(19.4)	
No	28(50.0)	89(61.4)	25(80.6)	
Typical enhancement				0.026
Yes	54(96.4)	128(88.3)	24(77.4)	
No	2(3.6)	17(11.7)	7(22.6)	
Cyst degeneration or necrosis				0.078
Yes	33(58.9)	104(71.7)	25(80.6)	
No	23(41.1)	41(28.3)	6(19.4)	
Quantitative indicators				
CT values in AP(Hu)	88.0±25.2	79.7±18.4	72.3±18.4	0.002
CT values in PVP(Hu)	87.7±15.4	81.9±13.3	74.0±16.2	<0.001
Maximum tumor length(mm)	81.7±11.4	77.4±11.1	70.9±12.4	0.008

significant difference ($P < 0.05$). There was no significant difference in the levels of albumin, total bilirubin, PLT, lymphocyte count, APTT, CA199, and CEA between the two groups ($P > 0.05$) (Table 5).

There were statistically significant differences in PLT, AFP levels, and MVI status among different differentiation groups ($P < 0.05$). There were no significant differences in AST, ALT, albumin, total bilirubin, ALBI score, lymphocyte count, PT, APTT, CA199, and CEA between groups ($P > 0.05$) (Table 6).

Multivariate Logistic Regression Analysis Results and Predictive Value of MVI

Using MVI status as the dependent variable, and combining the variables listed in Tables 1, 3, and 5 as independent variables, multivariate logistic regression analysis was conducted using stepwise regression. The results indicated that ALBI score, PT value, tumor capsule, and PVP CT value are independent risk factors for MVI occurrence in HCC patients ($P < 0.05$) (see Table 7).

The statistically significant indicators (ALBI score, PT value, PVP CT value, tumor capsule) selected from the multivariate logistic regression analysis were further analyzed using ROC curve analysis to assess their predictive performance for MVI occurrence (Figure 4). The study results demonstrated moderate to low predictive values (AUC values of 0.71, 0.58, 0.66, 0.60, respectively) for these indicators. Their combined application significantly improved predictive value (AUC value of 0.82) (Table 8).

In the multivariate logistic regression analysis, using AFP raw values or the cut-off value obtained from the ROC curve (300 ng/mL) showed no significant statistical difference between the two groups ($P > 0.05$).

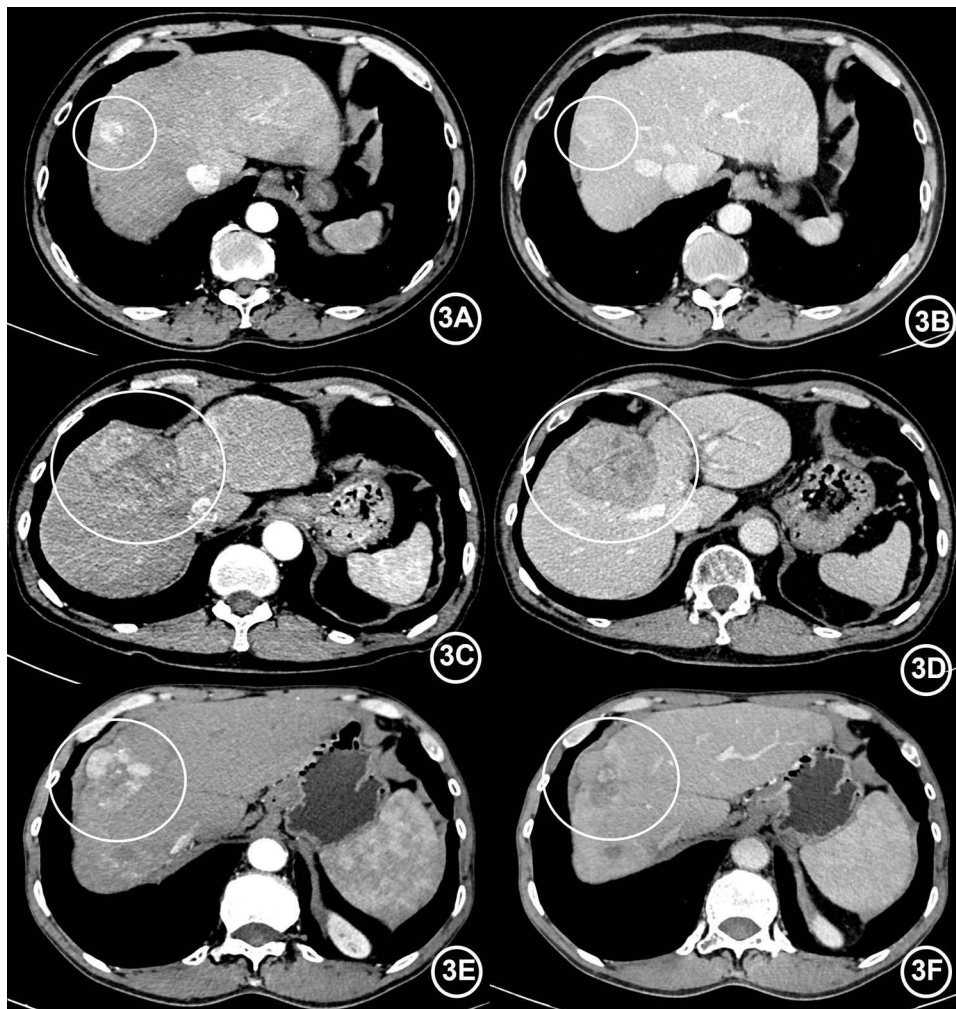


Figure 3 Differentiation-related imaging. (3A and 3B) A 70-year-old man with HCC, well differentiated. AP (3A) and PVP (3B) images show smooth tumor margin, tumor capsule, peritumoral enhancement, and typical enhancement pattern. The maximum tumor length is 33mm. The CT value in AP and PVP are 97Hu and 85Hu respectively. (3C and 3D) A 75-year-old man with HCC, moderately differentiated. AP (3C) and PVP (3D) images show smooth tumor margin, intratumoral artery, tumor capsule, cystic degeneration or necrosis, and typical enhancement pattern. The maximum tumor length is 64mm. The CT value in AP and PVP are 77Hu and 83Hu respectively. (3E and 3F) A 58-year-old man with HCC, poorly differentiated. AP (3E) and PVP (3F) images show irregular tumor margin, intratumoral artery, peritumoral enhancement, cystic degeneration or necrosis, and typical enhancement pattern. The maximum tumor length is 41mm. The CT value in AP and PVP are 101Hu and 79Hu respectively.

Results of Multivariate Logistic Regression Analysis of Pathological Grade

Selecting pathological grading as the dependent variable, and combining the variables listed in Tables 2, 4, and 6 as independent variables, a multivariate logistic regression analysis was conducted. The results showed that PVP CT value is an independent risk factor for different pathological grades in HCC patients ($P < 0.05$) (Table 9).

Table 5 Comparison of Clinical Characteristics Between the MVI (+) and MVI (-) Groups

Characteristics	MVI (+) (n=89)	MVI (-) (n=143)	Statistic	P value
AST (IU/L)	40(29.5, 59.5)	31(21, 51)	-3.127	0.002
ALT (IU/L)	35(23.5, 52.5)	29(18, 48)	-2.033	0.042
Albumin (g/L)	38.5(35.8, 41.0)	39.8(36.3, 42.4)	-1.690	0.093
Total bilirubin ($\mu\text{mol/L}$)	16.9(11.9, 22.6)	15(10.8, 21.2)	-1.219	0.223
ALBI score	-2.74 \pm 0.36	-2.45 \pm 0.41	-5.431	<0.001
PLT ($\times 10^9/\text{L}$)	133.0(99.5, 197.5)	129.5(89.8, 189.5)	-0.801	0.423

(Continued)

Table 5 (Continued).

Characteristics	MVI (+) (n=89)	MVI (-) (n=143)	Statistic	P value
Lymphocyte count	1.3(1.0, 1.6)	1.4(1.0, 1.7)	-1.183	0.237
PT (s)	11.7(11.2, 12.2)	11.9(11.4, 12.5)	-2.141	0.032
APTT (s)	28.3±2.0	28.1±2.1	-0.639	0.523
Tumor markers				
AFP (µg/mL)	39.6(4.64, 613.4)	1.4(4.0, 181.1)	-3.191	0.001
CA199 (ng/mL)	8.6(4.4, 21.8)	8.7(4.0, 14.0)	-1.346	0.178
CEA (ng/mL)	2.5(1.7, 3.5)	2.2(1.5, 3.4)	-0.836	0.403
Differentiation grade			7.226	0.027
Well	13(14.6)	43(30.1)		
Moderately	62(69.7)	83(58.0)		
Poorly	14(15.7)	17(11.9)		

Abbreviations: MVI, microvascular invasion; AST, aspartate aminotransferase; ALT, alanine aminotransferase; ALBI score, serum albumin-bilirubin score, PLT, platelet count; PT, prothrombin time; APTT, activated partial thromboplastin time; AFP, alpha-fetoprotein; CA199, cancer antigen 19-9; CEA, carcinoembryonic antigen.

Table 6 Comparison of Clinical Characteristics Between Well, Moderately, and Poorly Differentiation Groups

Characteristics	Well (n=56)	Moderately (n=145)	Poorly (n=31)	P value
AST (IU/L)	34.0(25.0, 51.8)	36.0(26.0, 55.5)	28.5(25.0, 55.0)	0.258
ALT (IU/L)	28.0(20.3, 43.5)	34.0(21.0, 50.5)	26.0(19.0, 38.0)	0.107
Albumin (g/L)	39.6±4.7	39.2±4.4	39.9±4.6	0.617
Total bilirubin (µmol/L)	16.2(12.7, 23.6)	15.2(11.3, 21.3)	11.6(9.2, 20.7)	0.078
ALBI score	-2.56±0.43	-2.54±0.41	-2.65±0.44	0.406
PLT (×10⁹/L)	123.5(77.3, 172.0)	126.5(92.0, 175.5)	195.0(121.0, 228.0)	0.001
Lymphocyte count	1.2(0.9, 1.6)	1.4(1.0, 1.7)	1.4(1.0, 1.9)	0.112
PT (s)	11.8(11.4, 12.4)	11.8(11.4, 12.5)	11.7(11.4, 12.1)	0.655
APTT (s)	28.0±1.9	28.3±2.2	28.2±2.0	0.759
Tumor markers				
AFP (µg/mL)	10.0(3.4, 146.7)	48.3(5.8, 627.4)	43.6(13.2, 955.4)	0.012
CA199 (ng/mL)	9.2(3.8, 14.2)	8.5(3.6, 18.0)	7.7(5.3, 17.1)	0.826
CEA (ng/mL)	2.5(1.7, 4.1)	2.3(1.7, 3.4)	2.1(1.7, 2.8)	0.456
MVI				0.037
Positive	13(23.2)	62(42.8)	14(45.2)	
Negative	43(76.8)	83(57.2)	17(54.8)	

Table 7 Results of Multivariate Logistic Regression Analysis of MVI Status

Factors	β	SE	Z	P	OR (95% CI)
ALBI score	2.06	0.46	4.45	<0.001	7.87 (3.17 ~ 19.53)
PT (s)	0.58	0.21	2.8	0.005	1.78 (1.19 ~ 2.68)
CT value in PVP (Hu)	0.04	0.01	3.02	0.002	1.04 (1.01 ~ 1.06)
Maximum length (mm)	-0.01	0.01	-1.47	0.141	0.99 (0.98 ~ 1.00)
Peritumoral enhancement	-0.81	0.44	-1.86	0.063	0.44 (0.19 ~ 1.04)
Tumor capsule	1.23	0.37	3.3	<0.001	3.42 (1.65 ~ 7.10)

Abbreviations: OR, odds ratio; 95% CI, 95% confidence interval.

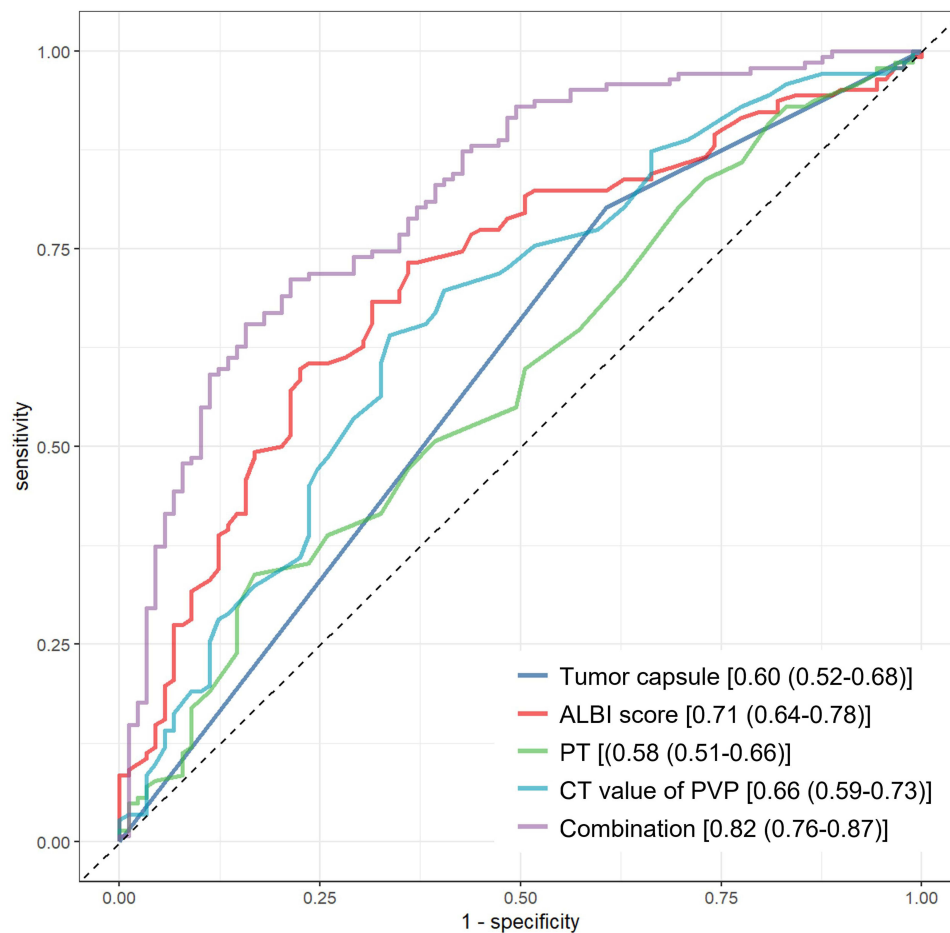


Figure 4 Receiver operating characteristic curve of MVI occurrence.

Discussion

This study retrospectively analyzed the clinical, pathological, and imaging data of 232 HCC patients. The results showed that there were some significantly different imaging and clinical features among groups with different pathological differentiation degrees and MVI statuses. This indicates that preoperative dynamic enhanced CT examination in HCC patients can be used to predict MVI status, among which the combination of clinical features and imaging features has a good predictive performance for MVI status and has important implications for the pathological differentiation degree of tumors. Previous studies have also proven the important potential of imaging features applied to preoperative MVI prediction, combining with clinical features can further improve the sensitivity and specificity of diagnosis.¹⁵⁻¹⁷

Table 8 The Predictive Value of Each Indicator for the Occurrence of MVI

Index	AUC (95% CI)	Cut-off	SEN	SPE	PPV	NPV	Yoden index
ALBI score	0.71(0.64–0.78)	–2.515	60	78	62	76	0.374
PT	0.58(0.51–0.66)	12.35	34	83	56	67	0.169
CT value in PVP	0.66(0.59–0.73)	81.5	64	66	54	75	0.304
Tumor capsule	0.60(0.52–0.68)	NA	80	61	56	83	0.196
Combination	0.82(0.76–0.87)	NA	66	84	72	80	0.498

Abbreviations: SEN, sensitivity; SPE, specificity; PPV, positive predictive value; NPV, negative predictive value; NA, not applicable.

Table 9 Results of Multivariate Logistic Regression Analysis of Pathological Grade

Differentiation*		SE	wald	P	OR (95% CI)
Well	CT value in PVP	0.032	4.941	0.026	1.07(1.01–1.14)
	ALBI score	0.761	1.291	0.256	2.37(0.53–10.56)
	Typical enhancement	0.972	1.404	0.236	3.17(0.47–21.29)
	Tumor capsule	0.662	2.514	0.113	2.86(0.78–10.46)
Moderately	CT value in PVP	0.029	4.033	0.045	1.06(1.01–1.12)
	ALBI score	0.667	0.825	0.364	1.83(0.50–6.77)
	Typical enhancement	0.661	0.343	0.558	1.47(0.40–5.37)
	Tumor capsule	0.546	1.758	0.185	2.06(0.71–6.01)

Note: *Compared to the poorly differentiated group.

Several studies have shown that imaging features such as irregular tumor margin, non-capsule, large tumor diameter, and peritumoral enhancement are closely related to MVI.^{18,19} The results of our study also showed that there were statistically significant differences in tumor margin, peritumoral enhancement, cystic degeneration or necrosis, tumor capsule, tumor diameter and CT values in arterial phase (AP) and PVP between MVI-positive and negative groups ($P < 0.05$). Multivariate logistic regression analysis showed that tumor capsule and CT values in PVP were independent predictors of MVI status. The tumor capsule structure mainly consists of an inner layer rich in fibrous components and an outer layer enveloping the portal vein and newly formed bile ducts. When tumor cells infiltrate and disrupt the capsule structure, imaging shows incomplete encapsulation and infiltrative border characteristics.^{18,20} The fibrous capsule of HCC is considered a favorable prognostic factor, associated with lower recurrence rates following more effective transarterial chemoembolization (TACE) and resection or ablation procedures, possibly due to the barrier effect of the fibrous capsule.^{20,21} The pathological results show that in areas where the capsule is missing, tumor cells are adjacent to normal liver cells, making it easier for tumor cells to infiltrate and invade surrounding vessels, thereby increasing the risk of MVI. Irregular tumor margins manifest as unclear boundaries with the hepatic parenchyma, nodular or mass-like external growth. The characteristics of tumor nodules are closely related to their blood supply status; tumors with exceptionally rich blood supply often exhibit more significant invasiveness. On imaging, such tumors show irregular and uneven edges with a nodular appearance, posing a higher risk of MVI, which most commonly occurs in the areas where nodules extend beyond the periphery.^{19,22} The pathological mechanism of peritumoral enhancement is closely related to compensatory arterial perfusion abnormalities in the liver. In cases of HCC with MVI, tumor cells invade and block intrahepatic microvascular structures, triggering compensatory adjustments in hepatic arterial blood flow.^{19,23} This compensatory perfusion anomaly is characterized by late arterial or early PVP enhancement of the peritumoral liver parenchyma, which decreases or disappears in the delayed phase (DP). Tumor size, as one of the important indicators for assessing HCC prognosis, is closely associated with MVI. The size of the tumor is not a definitive limiting factor for surgical resection or embolization therapy, but the risk of vascular invasion and tumor spread increases with increasing diameter.^{24,25} Studies^{8,20} have shown that tumor size is a key factor in the aggressiveness and prognostic outcome of HCC, with larger tumor volumes often indicating a higher incidence of MVI, which is consistent with our findings. Studies⁸ have shown that poorly differentiated tumors are associated with a higher incidence rate of MVI, which is consistent with our findings. Poorly differentiated HCC typically have dense and coarse tumor vessels, while well-differentiated HCCs have more abundant intrahepatic sinusoids, suggesting that well-differentiated HCCs may have more sources of venous blood supply compared to poorly differentiated HCC.²⁵ Our study found that the decrease in CT values in AP and PVP was associated with MVI positiveness and lower grade of differentiation. Multivariate logistic regression analysis showed that CT values in PVP were independent predictors of MVI and pathological differentiation. This may indicate that the risk of MVI increases with the decrease of the differentiation grade and blood supply especially the venous supply. Our study found that CT values in PVP were statistically significant in predicting pathological differentiation, but the increase in risk was relatively small (1.06, 1.07). Prospective studies are needed to evaluate its clinical significance.

AFP is the most commonly used serologic marker for screening HCC, but its sensitivity and specificity are only 60% and 80%, respectively.^{26,27} The results of this study showed that the preoperative serum AFP level in the MVI-positive group was significantly higher than that in the MVI-negative group, and the lower the degree of tumor differentiation, the higher the serum AFP levels ($P < 0.05$). However, in the multivariate logistic regression analysis, both the original AFP value and the cut-off value (300ng/mL) obtained by the ROC curve showed that there was no significant difference between the two groups ($P > 0.05$). This is inconsistent with the results of some studies¹⁸ and may be related to the lack of stratification. In fact, AFP levels in adult blood are affected by multiple factors, and other tests need to be combined to improve diagnostic or predictive efficiency. Research¹⁸ found that low PLT was a risk factor for preoperative MVI. However, our study did not find an association between PLT and MVI events. We found that higher PLT was associated with lower grade of differentiation, but no significant correlation was found in multivariate analysis. The conclusions of PLT analysis may need to be further discussed. The ALBI score is often used for preoperative assessment of liver function reserve and prognostic evaluation of postoperative liver failure after liver resection. Research²⁸ found that the recurrence rate of HCC transplantation significantly increased with the increase of ALBI grade, with ALBI grade 3 proven to be an independent predictor of MVI. The results of this study did not find a statistically significant relationship between albumin or total bilirubin and MVI and differentiation grade, but the ALBI score obtained from both was an independent predictor of MVI, which was consistent with the above study. The ALBI score may be a surrogate marker of inflammation and immune dysfunction in liver cirrhosis. Although the ALBI score has been shown to be effective in stratifying patients with HCC across different Barcelona Clinic Liver Cancer (BCLC) stages, its specific application value as a stratification tool in clinical practice or scientific research needs to be further clarified.²⁹

There were no statistically significant differences in liver cirrhosis and HBV infection among different MVI status or pathologic differentiation grade groups in this study, which is inconsistent with some studies.^{18,30} This inconsistency may be related to the presence of selection bias. Furthermore, the effect of HBV titer or viral load was not further analyzed in our study considering the impact of preoperative antiviral therapy.

The shortcomings of this study are mainly as follows: Firstly, it is a single-center retrospective study, and it is necessary to verify the results from other centers. Secondly, the study did not track postoperative recurrence and survival outcomes of patients. Thirdly, MVI was only classified into negative and positive groups without further grading. Fourthly, only macroscopic imaging information that can be obtained was used, without deep data mining. In the future, it is hoped to include a larger sample size and combine radiomics and deep learning to establish a predictive model for MVI grading, thereby improving overall predictive performance.

Conclusion

In summary, preoperative dynamic contrast-enhanced CT examinations in HCC patients can be used to predict MVI status and provide important hints regarding tumor pathological differentiation. The combination of clinical and radiological features shows good predictive performance for MVI status, which is highly valuable for guiding personalized treatment and further research.

Data Sharing Statement

All relevant data are available within the manuscript. Further enquiries can be directed to the corresponding author.

Ethics Statement

The study protocol was approved by the Ethics Committee of Sichuan Academy of Medical Sciences & Sichuan Provincial People's Hospital and conducted following the ethical principles outlined in the Helsinki Declaration of 1964 and its subsequent amendments, or other ethical standards with equivalent requirements. As a retrospective study as well as to ensure patient confidentiality, the identities of the individuals included in this study were anonymized using computer-generated ID numbers, and thus, patient consent was waived.

Author Contributions

All authors made a significant contribution to the work reported, whether that is in the conception, study design, execution, acquisition of data, analysis and interpretation, or in all these areas; took part in drafting, revising or critically reviewing the article; gave final approval of the version to be published; have agreed on the journal to which the article has been submitted; and agree to be accountable for all aspects of the work.

Funding

This work was funded by the University of Electronic Science and Technology of China, Sichuan Provincial People's Hospital "Medical-engineering Cross Joint Fund" (ZYGX2021YGLH213).

Disclosure

All authors have no relevant financial or non-financial interests to disclose for this work.

References

- Cao W, Chen HD, Yu YW, Li N, Chen WQ. Changing profiles of cancer burden worldwide and in China: a secondary analysis of the global cancer statistics 2020. *Chin Med J*. 2021;134(7):783–791. doi:10.1097/CM9.0000000000001474
- Gilles H, Garbutt T, Landrum J. Hepatocellular Carcinoma. *Rit Care Nurs Clin North Am*. 2022;34(3):289–301. doi:10.1016/j.cnc.2022.04.004
- Zhou J, Sun H, Wang Z, et al. Guidelines for the diagnosis and treatment of primary liver cancer (2022 edition). *Liver Cancer*. 2023;12(5):405–444. doi:10.1159/000530495
- Bray F, Ferlay J, Soerjomataram I, Siegel RL, Torre LA, Jemal A. Global cancer statistics 2018: GLOBOCAN estimates of incidence and mortality worldwide for 36 cancers in 185 countries. *Ca a Cancer J Clinicians*. 2018;68(6):394–424. doi:10.3322/caac.21492
- Chidambaranathan-Reghupaty S, Fisher PB, Sarkar D. Hepatocellular carcinoma (HCC): epidemiology, etiology and molecular classification. *Adv Cancer Res*. 2021;149:1–61. doi:10.1016/bs.acr.2020.10.001
- Forner A, Reig M, Bruix J. Hepatocellular carcinoma. *Lancet*. 2018;391(10127):1301–1314. doi:10.1016/S0140-6736(18)30010-2
- Rodríguez-Perálvarez M, Luong TV, Andreana L, Meyer T, Dhillon AP, Burroughs AK. A systematic review of microvascular invasion in hepatocellular carcinoma: diagnostic and prognostic variability. *Ann Surg Oncol*. 2012;20(1):325–339. doi:10.1245/s10434-012-2513-1
- Wang W, Guo Y, Zhong J, et al. The clinical significance of microvascular invasion in the surgical planning and postoperative sequential treatment in hepatocellular carcinoma. *Sci Rep*. 2021;11(1):2415.
- European Association for the Study of the Liver. European association for the study of the liver. EASL clinical practice guidelines: management of hepatocellular carcinoma [published correction appears in *J Hepatol*. 2019 Apr; 70(4):817]. *J Hepatol*. 2018;69(1):182–236. doi:10.1016/j.jhep.2018.03.019.
- Lee S, Kang TW, Song KD, et al. Effect of microvascular invasion risk on early recurrence of hepatocellular carcinoma after surgery and radiofrequency ablation. *Ann Surg*. 2021;273(3):564–571. doi:10.1097/SLA.000000000000326811
- Han DH, Choi GH, Kim KS, et al. Prognostic significance of the worst grade in hepatocellular carcinoma with heterogeneous histologic grades of differentiation. *J Gastroenterol Hepatol*. 2013;28(8):1384–1390. doi:10.1111/jgh.12200
- He X, Xu Y, Zhou C, et al. Prediction of microvascular invasion and pathological differentiation of hepatocellular carcinoma based on a deep learning model. *Eur J Radiol*. 2024;172:111348. doi:10.1016/j.ejrad.2024.111348
- Zheng Z, Guan R, Jianxi W, et al. Microvascular invasion in hepatocellular carcinoma: a review of its definition, clinical significance, and comprehensive management. *J Oncol*. 2022;2022:9567041. doi:10.1155/2022/9567041
- Cong WM, Bu H, Chen J, et al. Practice guidelines for the pathological diagnosis of primary liver cancer: 2015 update. *World J Gastroenterol*. 2016;22(42):9279–9287. doi:10.3748/wjg.v22.i42.9279
- Xu T, Ren L, Liao M, et al. Preoperative radiomics analysis of contrast-enhanced CT for microvascular invasion and prognosis stratification in hepatocellular carcinoma. *J Hepatocell Carcinoma*. 2022;9:189–201. doi:10.2147/JHC.S356573
- Zhang Z, Jia XF, Chen XY, Chen YH, Pan KH. Radiomics-based prediction of microvascular invasion grade in nodular hepatocellular carcinoma using contrast-enhanced magnetic resonance imaging. *J Hepatocell Carcinoma*. 2024;11:1185–1192. doi:10.2147/JHC.S461420
- Ryu T, Takami Y, Wada Y, et al. A clinical scoring system for predicting microvascular invasion in patients with hepatocellular carcinoma within the Milan criteria. *J Gastrointestinal Surg*. 2019;23(4):779–787. doi:10.1007/s11605-019-04134-y
- Lei Z, Li J, Wu D, et al. Nomogram for preoperative estimation of microvascular invasion risk in hepatitis B virus-related hepatocellular carcinoma within the Milan criteria. *JAMA Surgery*. 2016;151(4):356. doi:10.1001/jamasurg.2015.4257
- Renzulli M, Brocchi S, Cucchetti A, et al. Can current preoperative imaging be used to detect microvascular invasion of hepatocellular carcinoma? *Radiology*. 2016;279(2):432–442. doi:10.1148/radiol.2015150998
- Cho ES, Choi JY. MRI features of hepatocellular carcinoma related to biologic behavior. *Korean J Radiol*. 2015;16(3):449–464. doi:10.3348/kjr.2015.16.3.449
- Low HM, Lee JM, Tan CH. Prognosis prediction of hepatocellular carcinoma based on magnetic resonance imaging features. *Korean J Radiol*. 2023;24(7):660–667. doi:10.3348/kjr.2023.0168
- Jiang H, Wei J, Fu F, et al. Predicting microvascular invasion in hepatocellular carcinoma: a dual-institution study on gadoxetate disodium-enhanced MRI. *Liver Int*. 2022;42(5):1158–1172. doi:10.1111/liv.15231
- Matsui O, Kobayashi S, Sanada J, et al. Hepatocellular nodules in liver cirrhosis: hemodynamic evaluation (angiography-assisted CT) with special reference to multi-step hepatocarcinogenesis. *Abdominal Imaging*. 2011;36(3):264–272. doi:10.1007/s00261-011-9685-1

24. Liang BY, Gu J, Xiong M, et al. Tumor size may influence the prognosis of solitary hepatocellular carcinoma patients with cirrhosis and without macrovascular invasion after hepatectomy. *Sci Rep.* 2021;11(1):16343. doi:10.1038/s41598-021-95835-5
25. Hong SB, Choi SH, Kim SY, et al. MRI features for predicting microvascular invasion of hepatocellular carcinoma: a systematic review and meta-analysis. *Liver Cancer.* 2021;10(2):94–106. doi:10.1159/000513704
26. Marrero JA, Feng Z, Wang Y, et al. α -fetoprotein, des- γ carboxyprothrombin, and lectin-bound α -fetoprotein in early hepatocellular carcinoma. *Gastroenterology.* 2009;137(1):110–118. doi:10.1053/j.gastro.2009.04.005
27. Lok AS, Sterling RK, Everhart JE, et al. Des- γ -carboxy prothrombin and α -fetoprotein as biomarkers for the early detection of hepatocellular carcinoma. *Gastroenterology.* 2010;138(2):493–502. doi:10.1053/j.gastro.2009.10.031
28. Kornberg A, Witt U, Schernhammer M, et al. The role of preoperative albumin-bilirubin grade for oncological risk stratification in liver transplant patients with hepatocellular carcinoma. *J Surg Oncol.* 2019;120(7):1126–1136. doi:10.1002/jso.25721
29. Johnson PJ, Berhane S, Kagebayashi C, et al. Assessment of liver function in patients with hepatocellular carcinoma: a new evidence-based approach—the ALBI grade. *J clin oncol.* 2015;33(6):550–558. doi:10.1200/JCO.2014.57.9151
30. Wei X, Li N, Li S, et al. Hepatitis B virus infection and active replication promote the formation of vascular invasion in hepatocellular carcinoma. *BMC Cancer.* 2017;17(1). doi:10.1186/s12885-017-3293-6.

Journal of Hepatocellular Carcinoma

Publish your work in this journal

The Journal of Hepatocellular Carcinoma is an international, peer-reviewed, open access journal that offers a platform for the dissemination and study of clinical, translational and basic research findings in this rapidly developing field. Development in areas including, but not limited to, epidemiology, vaccination, hepatitis therapy, pathology and molecular tumor classification and prognostication are all considered for publication. The manuscript management system is completely online and includes a very quick and fair peer-review system, which is all easy to use. Visit <http://www.dovepress.com/testimonials.php> to read real quotes from published authors.

Submit your manuscript here: <https://www.dovepress.com/journal-of-hepatocellular-carcinoma-journal>

Dovepress
Taylor & Francis Group